Effect of the Electrode Continuum of States in Adiabatic and Nonadiabatic Outer-Sphere and Dissociative Electron Transfers. Use of Cyclic Voltammetry for Investigating Nonlinear Activation-Driving Force Laws

Jean-Michel Savéant†

Laboratoire d'Electrochimie Moléculaire, Unité Mixte de Recherche Université - CNRS No 7591, Université de Paris 7 - Denis Diderot, 2 place Jussieu, 75251 Paris Cedex 05, France

Received: March 25, 2002

The impact of taking into account the multiplicity of electrode electronic states on the kinetics of outer-sphere and dissociative electron transfers is discussed under the approximation that the electronic coupling energy and the density of states are not strongly dependent on the energy of the electronic states with emphasis on practical consequences. It is shown that, in most cases of practical interest, the activation-driving force laws may be derived from the classical Marcus−Hush quadratic relationship by application of a simple and small correction. Under the same approximation, the passage from adiabatic to fully nonadiabatic behaviors can be estimated as a function of the electronic coupling energy, showing that the reaching of complete adiabaticity requires rather modest values of this factor. In the same pragmatic vein, we discuss how cyclic voltammetry can be used to derive nonlinear kinetic laws from experimental data. It is often believed that the extraction of kinetic information from the cyclic voltammetric raw data requires that the form of the kinetic law be known a priori, consequently causing a preference for potential-step or impedance techniques where this question does not arise. It will be shown that simple treatments of the raw data, both in the case where the reactants are attached to the electrode surface or free to move in the solution, can be used to circumvent this apparent difficulty making cyclic voltammetry a tool as efficient as the above-mentioned techniques for this purpose.

Introduction

Albeit the effect of the presence of many electronic energy levels in the electrode on electrochemical electron-transfer kinetics has been discussed for a long time,[1] most experimental studies have relied on a version of Marcus−Hush theory[2,3] in which most electrons that are transferred to or from the many-electrons energy levels in the electrode behave as if they go into or from the Fermi level.[2b] More recently, attachment of redox molecules, by means of self-assembled monolayers, [4] has been the occasion of revisiting this question from an experimental standpoint, at least in the framework of nonadiabatic electron transfers.[5] One difficulty of the application of the MHL (Marcus, Hush, Levich) theory in this case is the possible dependence of the rate of electron transfer from the density and nature of the electronic states.[6,7] Recent quantum chemical estimations comparing gold and platinum have, however, shown that the electronic coupling energy and the density of states are not strongly dependent on the energy of the electronic states, at least for these systems and within the degree of confidence of the quantum chemical methods used.[7]

Under this approximation, the treatment of adiabatic and nonadiabatic reactions may be unified and the passage from one situation to the other described. An interesting outcome of such an analysis is the prediction of the value of the electronic coupling energy that would make the reaction adiabatic or completely nonadiabatic as a function of the reorganization energy attending electron transfer. Experimental systems made of attached redox molecules, falling in the nonadiabatic category, have been analyzed according to the MHL model, clearly showing the variation of the transfer coefficient with the electrode potential.[5] The results obtained earlier with a series of free-moving organic molecules, also showing a definite variation of the transfer coefficient with potential[8] are worth reexamining in the framework of the MHL model. Application to dissociative electron transfer is also deemed important because the variation of the transfer coefficient with the driving force has been shown to be a potent tool in mechanism analysis.[9]

The resulting activation-driving force laws are definitely more complex than the traditional Marcus−Hush quadratic relationship. Useful polynomial expressions have accordingly been proposed in this connection.[10] It is even more interesting to estimate what error would be made if a second order fitting were attempted, i.e., if the activation-driving force relationship were approximated by a quadratic expression of the same form as used for the individual rate constants. The neglect of the error or, if necessary, the use of a simple correction procedure would considerably ease analyses and predictions concerning experimental systems. These various questions are discussed in the following sections, noting that they arise not only in the case of outer-sphere electron transfers but in the case of dissociative electron transfers as well.

Pursuing in the same pragmatic vein, we will examine how cyclic voltammetry can be used to derive nonlinear kinetic laws from the experimental data. It is often believed that the extraction of kinetic information from the cyclic voltammetric raw data requires that the form of the kinetic law be known a priori, consequently causing a preference for potential-step or impedance techniques where this question does not arise.[5,11] It will be shown that simple treatments of the raw data can be used to circumvent this apparent difficulty, making cyclic

† E-mail: saveant@paris7.jussieu.fr.

10.1021/jp0258006 CCC: $22.00
Published on Web 08/16/2002

voltammetry a tool as efficient as the above-mentioned techniques for this purpose.

Effect of the Multiplicity of Electronic States in the Electrode

Considering a simple outer-sphere electron-transfer reaction

$$A^{z_A} + e^- \rightleftharpoons B^{(z_A-1)}$$

(z_A, charge number of the reactant), the rate law may be expressed by the following relationships, in which the forward and backward rate constants, k_f and k_b, are functions of the potential E of the electrode.

$$\frac{i}{FS} = k_f(E)(C_A)_0 - k_b(E)(C_B)_0 = k_f(E)\left\{(C_A)_0 - \exp\left[\frac{F}{\mathscr{R}T}(E - E^0)\right](C_B)_0\right\} \quad (1)$$

(F, faraday; S, electrode surface area; $(C_A)_0$ and $(C_B)_0$ are the concentrations of the reactants A and B at the electrode surface), or alternatively

$$\frac{i}{FS} = k_f^{het}(E)\Gamma_A - k_b^{het}(E)\Gamma_B = k_f^{het}(E)\left\{\Gamma_A - \Gamma_B \exp\left[\frac{F}{\mathscr{R}T}(E - E^0)\right]\right\} \quad (2)$$

(Γ_A and Γ_B are the surface concentrations of the reactants A and B).

The first formulation is more directly suited to the case of reactants in solution, and the second, to attached reactants. In the first case, the rate constants have the dimension of a length time^{-1}, typically cm s^{-1}, whereas, in the second case, they have the dimension of a time^{-1}, typically s^{-1}.

The individual forward rate constant for the transfer, $k_{f,j}$, of one electron from one electron state (j) in the metal to the acceptor (oxidized form of the redox couple) in the solution may be expressed as ($\mathscr{R}$ and $\mathscr{k}$, gas and Boltzmann constants respectively)

$$k_{f,j} = Z^{el}\kappa_{el,j}\exp\left(-\frac{F\Delta G^{\ddagger}_{f,j}}{\mathscr{R}T}\right) \quad \text{for the first formulation}$$

and

$$k_{f,j}^{het} = \frac{\mathscr{k}T}{h}\kappa_{el,j}\exp\left(-\frac{F\Delta G^{\ddagger}_{f,j}}{\mathscr{R}T}\right) \quad \text{for the second formulation}$$

The preexponential factor Z^{el} may be derived from the collision frequency of a particle against a plane, or equivalently, in the framework of transition state theory, from the ratio of the partition functions of the transition state and the initial state of the reactant:[12]

$$k_\infty = Z^{el} = \sqrt{\frac{\mathscr{R}T}{2\pi M}}$$

(M, molar mass of the reactant). $\kappa_{el,j}$ is the transmission coefficient corresponding to the electronic state j. Its value is related to the degree of adiabaticity, as discussed in the next section.

The individual activation free energy for the forward reaction, $\Delta G^{\ddagger}_{f,j}$, is related to the reorganization energy, λ, according to

$$\Delta G^{\ddagger}_{f,j} = \frac{\lambda}{4}\left(1 - \frac{\mathbf{E} - \mathbf{E}^0}{\lambda}\right)^2 = \frac{1}{4\lambda}[\lambda - (\mathbf{E} - \mathbf{E}^0)]^2 \quad (3)$$

($\mathbf{E}$ is the energy of the electron in the metal, and $\mathbf{E}°$, its value when the electrode potential, E, is equal to the formal potential of the redox couple, $E°$). The overall rate constant, k_f, is obtained after multiplication by the Fermi−Dirac probability of finding an electron with the energy $\mathbf{E}$, namely

$$\frac{1}{1 + \exp\left[\frac{F}{\mathscr{R}T}(\mathbf{E} - \mathbf{E}_F)\right]}$$

by integration over the whole set of electron states in the metal, under the approximation mentioned in the Introduction (see Appendix):

$$k_f(E) = \frac{k_\infty}{\sqrt{4\pi\lambda}}\int_{-\infty}^{\infty}\frac{\exp\left[-\frac{\mathscr{R}T}{4F\lambda}\left\{\frac{F}{\mathscr{R}T}[\lambda + (E - E^0)] - \zeta\right\}^2\right]}{1 + \exp(\zeta)}\,d\zeta = \frac{k_\infty}{\sqrt{\pi}}\int_{-\infty}^{\infty}\frac{\exp(-\upsilon^2)\,d\upsilon}{1 + \exp\left\{\frac{F}{\mathscr{R}T}[\lambda + (E - E^0)]\right\}\exp(\sqrt{4\lambda}\upsilon)} \quad (4)$$

Similarly, for the reverse reaction

$$k_{b,j} = Z^{el}\kappa_{el,j}\exp\left(-\frac{F\Delta G^{\ddagger}_{b,i}}{\mathscr{R}T}\right)$$

The individual activation free energy for the backward reaction, $\Delta G^{\ddagger}_{b,j}$, is related to the reorganization energy, λ, according to

$$\Delta G^{\ddagger}_{b,j} = \frac{\lambda}{4}\left(1 + \frac{\mathbf{E} - \mathbf{E}^0}{\lambda}\right)^2 = \frac{1}{4\lambda}[\lambda + (\mathbf{E} - \mathbf{E}^0)]^2 \quad (5)$$

The overall rate constant, k_b, is obtained after multiplication by the Fermi−Dirac probability of finding a hole with the energy $\mathbf{E}$, namely

$$\frac{1}{1 + \exp\left[-\frac{F}{T}(\mathbf{E} - \mathbf{E}_F)\right]}$$

by integration over the whole set of holes states in the metal

$$k_b(E) = \frac{k_\infty}{\sqrt{4\pi\lambda}}\int_{-\infty}^{\infty}\frac{\exp\left[-\frac{\mathscr{R}T}{4F\lambda}\left\{\frac{F}{\mathscr{R}T}[\lambda - (E - E^0)] - \zeta\right\}^2\right]}{1 + \exp(\zeta)}\,d\zeta = \frac{k_\infty}{\sqrt{\pi}}\int_{-\infty}^{\infty}\frac{\exp(-\upsilon^2)\,d\upsilon}{1 + \exp\left\{\frac{F}{T}[\lambda - (E - E^0)]\right\}\exp(\sqrt{4\lambda}\upsilon)} \quad (6)$$

and, at zero driving force ($E = E^0$):

$$k_S = \frac{k_\infty}{\sqrt{4\pi\lambda}}\int_{-\infty}^{\infty}\frac{\exp\left[-\frac{T}{4F\lambda}\left(\frac{F\lambda}{\mathscr{R}T} - \zeta\right)^2\right]}{1 + \exp(\zeta)}\,d\zeta \quad (7)$$

Equations 4, 6, and 7 may be used in the rate expressed by eq 1, making

$$k_\infty = Z^{el}\kappa_{el}$$

and in the other expression of the rate law (eq 2), making

$$k_{\infty}^{\text{het}} = \frac{T}{h}\kappa_{\text{el}}$$

The same derivations apply to *dissociative electron transfers*

$$RX \pm e^{-} \rightharpoonup R^{\bullet} + X^{\mp}$$

because application of the Morse curve semiclassical model to the individual rate constants leads to quadratic expressions similar to eqs 3 and 5, where the reorganization energy, λ, now includes the bond dissociation energy of RX, besides the solvent reorganization energies and energies pertaining the reorganization of noncleaving bonds.[13]

It follows that eqs 4, 6, amd 7 and all the following analyses and conclusions apply to these reactions too.

Adiabatic vs Nonadiabatic Electron Transfers

The Marcus−Hush model used for the individual rate constants is based on the intersection of two diabatic potential energy surfaces. However, there should be some mixing of the two states at the intersection for electron transfer to occur. Otherwise, coming from the initial reactant state, the system would remain on the same diabatic surface, thus preventing the conversion of reactant into product. The probability, $P_{‡}$, that the reactant be converted into product on passing over the activation barrier is an increasing function of the electronic coupling energy, H, between the two states at the intersection of the two diabatic surfaces. When resonance between the two states at the transition state is sufficient for the reaction probability to reach unity, the reaction is said to be adiabatic. Then

$$k_{\infty} = Z^{\text{el}} = \sqrt{\frac{\mathcal{R}T}{2\pi M}} \qquad \text{and} \qquad k_{\infty}^{\text{het}} = \frac{\not{k}T}{h}$$

The probability $P_{‡}$ may be related to H by application[14] of the Landau−Zener model.[15,16]

$$P_{‡} = 1 - \exp\left[-\frac{\pi^{3/2}H^2}{\lambda^{1/2}}\left(\frac{F}{\mathcal{R}T}\right)^{3/2}\right]$$

This expression is valid for each individual rate constant but also for the overall rate constants given by eqs 4, 6, and 7 under the assumption that the electronic coupling energy is independent of the energy of the electronic state.

The preexponential factors, k_{∞} and k_{∞}^{h} may therefore be factorized by introduction of the electronic transmission coefficient, κ_{el}:

$$k_{\infty} = Z^{\text{el}}\kappa_{\text{el}} \qquad \text{or} \qquad k_{\infty}^{\text{het}} = \frac{\not{k}T}{h}\kappa_{\text{el}}$$

with

$$\kappa_{\text{el}} = \frac{2P_{‡}}{1 + P_{‡}}$$

i.e.,

$$\kappa_{\text{el}} = \frac{2 - 2\exp\left[-\frac{\pi^{3/2}H^2}{\lambda^{1/2}}\left(\frac{F}{\mathcal{R}T}\right)^{3/2}\right]}{2 - \exp\left[-\frac{\pi^{3/2}H^2}{\lambda^{1/2}}\left(\frac{F}{T}\right)^{3/2}\right]}$$

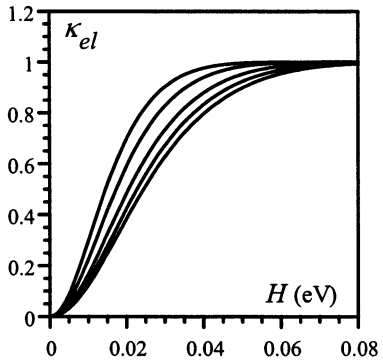

Figure 1. Passage from nonadiabatic to adiabatic conditions. Variations of the transmission coefficient with the electronic coupling energy, H, for various values of the reorganization energy. From left to right: λ = 0.5, 1, 2, 3, 4 eV. Temperature: 25 °C.

When H is small, the exponential may be developed to first order, leading to

$$\kappa_{\text{el}} = \frac{\pi^{3/2}H^2}{\lambda^{1/2}}\left(\frac{F}{T}\right)^{3/2}$$

Under these conditions, electron transfer is traditionally called *nonadiabatic*.

In the adiabatic limit, the electronic coupling (or resonance, or avoided crossing) energy, H, should, strictly speaking, be subtracted from the activation free energy derived from the crossing of the diabatic surfaces. In a number of cases, however, H is small enough for this correction to be negligible yet large enough for adiabaticity to be ensured. The continuous passage from a nonadiabatic to an adiabatic behavior is illustrated in Figure 1 by the variations of the transmission coefficient with H, for several values of the reorganization energy, λ. It is indeed seen that full adiabaticity does not require a large value of H to be reached. In contrast, when electron transfer is forced to take place at a large distance from the electrode by means of an appropriate spacer, the reaction quickly falls within the nonadiabatic limit. H is then a strongly decreasing function of distance. Several models predict an exponential decrease of H_{AB} with distance with a coefficient of the order of 1 Å^{-1}.[17]

Quadratic Approximation of the Rate Laws

An example illustrating the difference between the activation/driving force relationships for the individual and the overall rate constants is shown in Figure 2a. The most striking difference is the vanishing of the "inverted region" from the individual to the overall rate constant curves. Before the apex of the parabolas the difference in the curves is rather modest. Attempting a quadratic approximation of the curves (Figure 2b) within this driving force range leads to the results summarized in Figure 2c,d.

Concerning the standard rate constant, or equivalently, the intrinsic barrier, Figure 2c shows that the latter is still proportional to the reorganization energy, λ, and that the proportionality factor $^1/_4$ has simply to be multiplied by 1.07. Figure 2d shows that the quadratic approximation holds quite satisfactorily in driving force ranges of practical interest (i.e., $0 \geq E - E^0 \geq -\lambda$ for reduction and $0 \leq E - E^0 \leq \lambda$ for oxidation), except for very low values of λ. The following expressions may therefore be used in practice with negligible

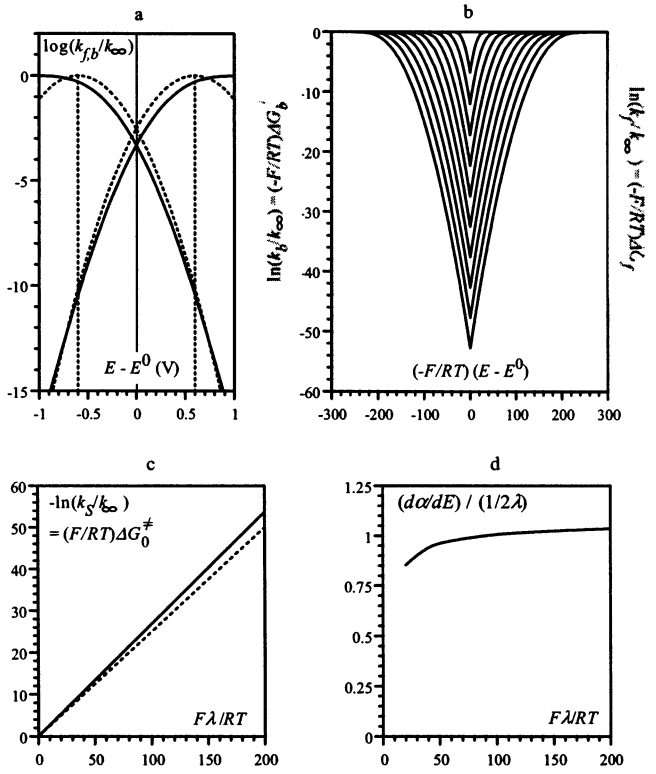

Figure 2. Quadratic approximation of the rate laws. (a) Comparison of the activation/driving force relationships for the individual (dotted lines) and the overall (full lines) rate constants ($\lambda = 0.6$ eV, temp 25 °C). (b) Variation of the forward and backward rate constants with the driving force as a function of the reorganization energy (from top to bottom: $\mathscr{R}TT\lambda/F = 20, 40, 60, 80, 100, 120, 140, 160, 180, 200$). (c) Variation of the intrinsic barrier with the reorganization energy for the overall (full lines) and individual (dotted lines) rate constants. (d) Variation of the transfer coefficient with potential as a function of the reorganization energy for the overall (full lines) and individual (dotted lines) rate constants.

error as substitutes for eqs 4, 6, and 7, thus easing analyses and predictions.

$$\Delta G_f^{\ddagger} = \frac{1.07\lambda}{4}\left(1 + \frac{E - E^0}{1.07\lambda}\right)^2 \tag{8}$$

$$\Delta G_b^{\ddagger} = \frac{1.07\lambda}{4}\left(1 - \frac{E - E^0}{1.07\lambda}\right)^2 \tag{9}$$

In the framework of the same approximation, the variation of the transfer coefficient with potential is given by

$$\alpha = 0.5\left(1 + \frac{E - E^0}{1.07\lambda}\right) \tag{10}$$

Double Layer Effect on the Electron-Transfer Kinetics (Frumkin Correction)

In the above expressions of the driving force, E, is, strictly speaking, the potential difference between the electrode and the reaction site. It is usually not exactly the same as the potential difference between the electrode and the solution. A commonly accepted assumption is that the reaction site is located in the outer Helmoltz plane of the double layer where the electrical potential, traditionally noted ϕ_2, is not the same as in the bulk of the solution. The usefulness of this assumption resides in the fact that ϕ_2 can be derived from current models of the electrochemical double layer.[18] At potentials more negative than the point of zero charge, ϕ_2 is negative and therefore less driving force is offered to the reduction than expected from the nominal value of E. Likewise, at potentials more positive than the point of zero charge, ϕ_2 is positive, entailing a lesser driving force for oxidation. The value of ϕ_2 depends on the concentration of supporting electrolyte. At concentrations of the order of 0.1 M, as those typically used in molecular electrochemistry experiments, the maximal value of ϕ_2 are of the order of 100 mV in absolute value.

Because the reactant and/or the product are charged species, the fact that the electrical potential in the solution and at the reaction site is not the same leads to the introduction of "work terms",

$$w_A = z_A\phi_2 \qquad \text{for the reactants}$$

$$w_B = (z_A - 1)\phi_2 \qquad \text{for the products}$$

which measure the free energy required to bring the reactant and the product, respectively, from the bulk of the solution to the reaction site. Apparent forward and backward activation free energies are consequently introduced, related to the "true" activation free energies by

$$\Delta G_{f,ap}^{\ddagger} = w_A + \Delta G_f^{\ddagger} \qquad \Delta G_{b,ap}^{\ddagger} = w_B + \Delta G_b^{\ddagger}$$

implying that $\Delta G^\circ = E - E^0$ is replaced by $\Delta G^\circ - w_A + w_B$ in the expression of the driving force.

It follows that k_S in eq 5 is converted into

$$k_S^{ap} = k_S \exp\left(-\frac{z_A F}{\mathscr{R}T}\phi_2\right)$$

Likewise, k_f^{ap} and k_b^{ap} are obtained from eqs 3 and 4 by the introduction of the terms $\exp(-z_A F/T\phi_2)$ and $\exp(-z_B F/T\phi_2)$, respectively, in the pre-integral factor and by replacement of E^0 by $E^0 + \phi_2$.

Using Cyclic Voltammetry in the Investigation of Nonlinear Activation-Driving Force Laws

As an example of a nonlinear activation-driving force law, typical cyclic voltammograms obtained with MHL kinetics are shown in Figure 4a in the case of *attached reactants*. The problem may be addressed at two levels of precision. (i) A quick and approximate procedure may be used if the nonlinear character of the activation-driving force law is not very pronounced so that it may be neglected within the relatively narrow potential range over which the voltammetric signal extends itself at a given scan rate. The nonlinear character of the activation-driving force law, or equivalently, the variation of α with potential, if any, will then appear upon comparison of the responses obtained at different scan rates. (ii) A more accurate approach consists of deriving the activation-driving force law, and evidence its nonlinear character, by appropriate manipulations of the raw data, with no a priori assumptions about the form of the law.

(i) Because the passage from reversibility to complete irreversibility also occurs over a narrow potential range, we may concentrate on completely irreversible signals. Under these conditions, the electrode potential may thus be expressed as

$$E = E_p + \Delta E$$

introducing a narrow potential excursion, ΔE, around the peak potential, E_p. Because the transfer coefficient is a constant, equal

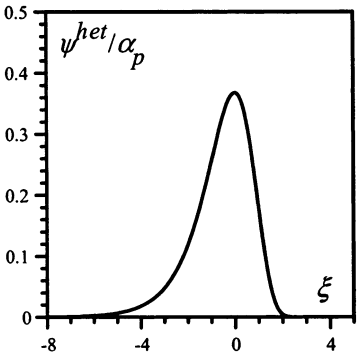

Figure 3. Attached reactants. Irreversible cyclic voltammetric surface wave obeying a linearized activation/driving force law (eq 12).

to its value at the peak, α_p, within this potential range, the rate law may be expressed as

$$\frac{i}{FS} = k_f^{het}(E)\Gamma_A = k_\infty^{het}\exp\left[-\frac{F}{\mathcal{R}T}(\Delta G_{f,p}^{\ddagger} + \alpha_p \Delta E)\right]\Gamma_A$$

where $\Delta G_{f,p}^{\ddagger}$ is the free energy of activation of the forward reaction at the peak potential, and

$$\Gamma_A = \Gamma^0 - \int_0^t \frac{i}{FS}\,dt$$

Defining

$$\xi = -\frac{\alpha_p F}{\mathcal{R}T}\Delta E + \ln\left(\frac{\mathcal{R}T k_\infty^{het}}{\alpha F\ v}\right) - \frac{F}{\mathcal{R}T}\Delta G_{f,p}^{\ddagger} \qquad (11)$$

$$\psi^{het} = \frac{i}{FS\Gamma^0 \frac{Fv}{T}}$$

(Γ^0, total surface concentration of reactant; v, scan rate), and noting that during the cathodic scan

$$\frac{d\xi}{dt} = \frac{Fv}{RT}$$

$$\frac{\psi^{het}}{\alpha_p}\exp(-\xi) = \left(1 - \int_{-\infty}^{\xi}\frac{\psi^{het}}{\alpha_p}\,d\eta\right)$$

lead to[19]

$$\frac{\psi^{het}}{\alpha_p} = \exp(-\xi)\exp[-\exp(-\xi)] \qquad (12)$$

As shown in Figure 3, this is a peak-shaped curve with the following characteristics.

$$\psi_p^{het}/\alpha_p = 0.368 \qquad \xi_p = 0$$

$$\Delta\xi_p = 2.46 \text{ (total width at } \psi^{het} = \psi_p^{het}/2)$$

It follows from the fact that $\xi_p = 0$ and from eq 11 that

$$\Delta G_{f,p}^{\ddagger} = \frac{\mathcal{R}T}{F}\ln\left(\frac{\mathcal{R}T}{\alpha_p F}\frac{k_\infty^{het}}{v}\right) \quad \text{or} \quad k_f^{het}(E_p) = \frac{\alpha_p F v}{T}$$

The free energy of activation or the forward rate constant may thus be obtained as a function of E_p for each scan rate. The nonlinear character of the rate law, if any, will then appear in the variation of $\Delta G_{f,p}^{\ddagger}$ with the peak potential, which provides a point-by-point depiction of the activation driving force relationship (one point per scan rate). The nonlinear character of the rate law will also transpire in the variation of α_p, derived from

$$\alpha_p = 2.42\frac{\mathcal{R}T}{F(E_{p/2} - E_p)}$$

with the scan rate.

(ii) If the nonlinear character of the kinetic law is more pronounced, and/or if more data points than merely the peak are to be used, the following approach, illustrated in Figure 4, may be used. The current−time curves are first integrated so as to obtain the surface concentrations of the two reactants. The

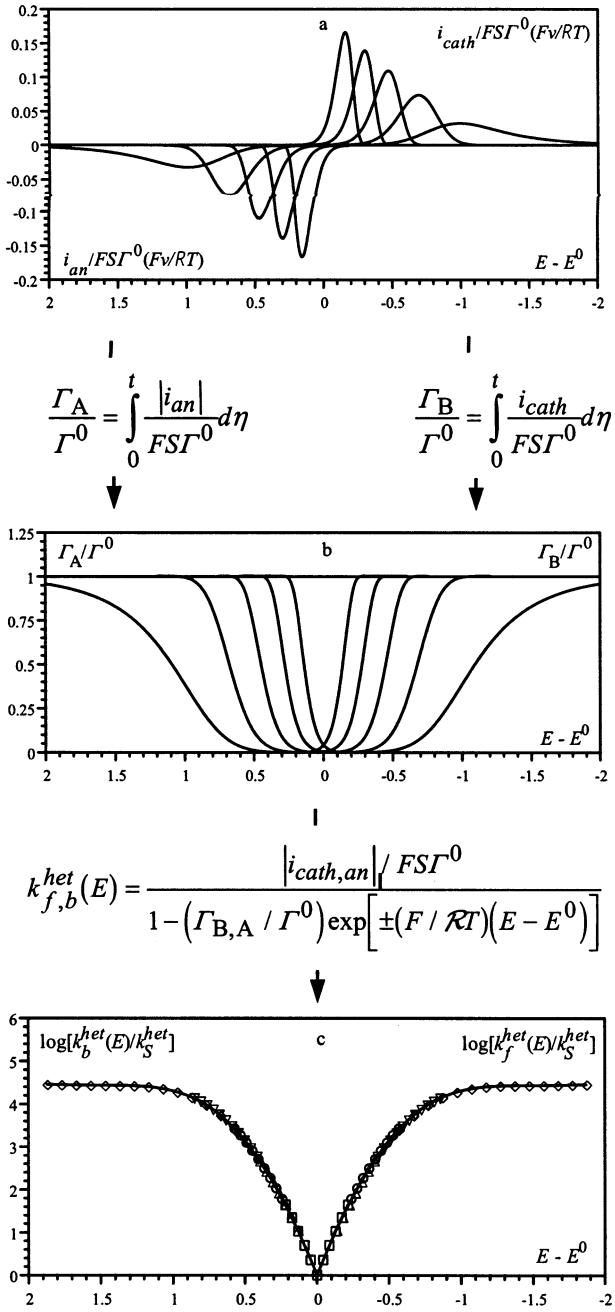

Figure 4. Deriving the rate law of an electron-transfer involving immobilized reactants from the cyclic voltammetric responses. (a) Voltammograms recorded at 1 (□), 10 (△), 100 (○), 1000 (▽), 10 000 (◇) V/s. (b) Derivation of the surface concentrations from the current responses. (c) Potential-dependent rate constant from the combination of a and b. $\lambda = 0.85$ eV and a standard rate constant $k_S^{het} = 1\ s^{-1}$.

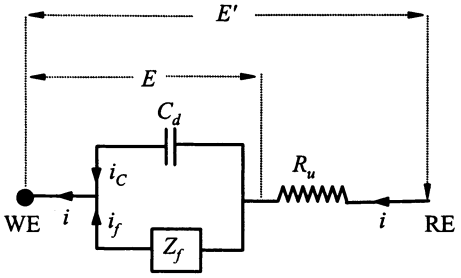

Figure 5. Working electrode (WE) equivalent circuit. Key: RE, reference electrode; C_d, double layer capacitance; Z_f, faradaic impedance; R_u, uncompensated resistance; i_C, double layer charging current; i_f, faradaic current; i, total current; E, potential difference across the faradaic impedance; E', potential difference between the working and reference electrodes.

current and the surface concentrations are then combined to derive the forward and backward rate constants as functions of the electrode potential. Following this strategy, the form of the dependence of the rate constants from potential need not to be known a priori. It is rather an outcome of the cyclic voltammetric experiments and of their treatment. There is therefore no compulsory need, as often believed, to use in this purpose electrochemical techniques in which the electrode potential is independent of time, or nearly independent of time, as in potential step chronoamperometry and impedance measurements. This is another illustration of the equivalence of the various electrochemical techniques provided they are used in comparable time-windows.

For the sake of a better readability, the variations of the two rate constants in Figure 4 have been restricted to the values between the standard rate constant, k_S^{het}, and the maximal rate constant, k_∞^{het}. Prolongations toward smaller values are readily obtained by application of the Nernst law. The example chosen to illustrate the procedure for extracting the kinetic law from the raw data is an electron-transfer reaction obeying the MHL model (eqs 4, 6, and 7) with a reorganization energy $\lambda = 0.85$ eV and a standard rate constant $k_S^{het} = 1\ s^{-1}$.

The preceding derivation implicitly assumed that the double layer charging current is negligible in front of the faradaic current or that it can be eliminated by a simple subtraction procedure. In cases where these conditions are not fulfilled, the following treatment will take care of the problem under the assumption that the double layer capacitance is not appreciably affected by the faradaic reaction but may nevertheless vary in the potential range explored. The first step of the treatment then consists of extracting the faradaic component from the total current according to the equivalent circuit in Figure 5according to

$$i_f = i + C_d\frac{dE'}{dt} + R_u C_d\frac{di}{dt} \qquad (13)$$

after the double layer capacitance has been determined in a blank experiment. The previously described procedure is then applied to the faradaic current thus extracted from the raw data.

Similar approaches may be followed in the case of *free moving reactants*.

(i) Linearization may likewise be attempted if the transfer coefficient does not vary significantly along each of the voltammograms taken at various scan rates although it may vary from one voltammogram to the other. Concentrating again on completely irreversible signals, the rate law may be expressed as

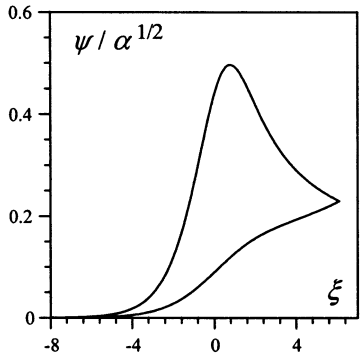

Figure 6. Free moving reactants. Irreversible cyclic voltammetric surface wave obeying a linearized activation/driving force law (eq 14).

$$\frac{i}{FS} = k_f(E)(C_A)_0 = k_\infty \exp\left[-\frac{F}{\mathcal{R}T}(\Delta G_{f,p}^{\ddagger} + \alpha_p \Delta E)\right](C_A)_0$$

after introduction, as before, of a narrow potential excursion, ΔE, around the peak potential, E_p

$$E = E_p + \Delta E$$

thanks to the assumption that the transfer coefficient, α_p, may be considered as a constant within this potential range, $\Delta G_{f,p}^{\ddagger}$ being the free energy of activation of the forward reaction at the peak potential.

Defining

$$\xi = -\frac{\alpha_p F}{\mathcal{R}T}\Delta E + \ln\left(k_\infty\sqrt{\frac{\mathcal{R}T}{\alpha F v D}}\right) - \frac{F}{T}\Delta G_{f,p}^{\ddagger} \qquad (14)$$

the following dimensionless voltammogram is obtained:[20]

$$\frac{\psi}{\sqrt{\alpha_p}}\exp(-\xi) = \left(1 - \frac{1}{\sqrt{\pi}}\int_{-\infty}^{\xi}\frac{\psi}{\sqrt{\alpha_p}}\frac{d\eta}{\sqrt{\xi - \eta}}\right)$$

with

$$\psi = \frac{i}{FSC^0\sqrt{D}\sqrt{\frac{Fv}{T}}}$$

(C^0, bulk concentration of A; D, diffusion coefficient).

As shown in Figure 6, this is a peak-shaped curve with the following characteristics.

$$\psi_p^{het}/\alpha_p = 0.368 \qquad \xi_p = 0.78 \qquad \Delta\xi_p = \xi_p - \xi_{p/2} = 1.857$$

Because $\xi_p = 0.78$ and $\Delta E = 0$ at the peak, it follows from eq 14 that

$$\Delta G_{f,p}^{\ddagger} = \frac{\mathcal{R}T}{F}\left[\ln\left(k_\infty\sqrt{\frac{\mathcal{R}T}{\alpha_p F v D}}\right) - 0.78\right]$$

or

$$k_f(E_p) = 0.78\sqrt{\frac{\alpha_p F v D}{\mathcal{R}T}}$$

The free energy of activation or the forward rate constant may thus be obtained as a function of E_p at each scan rate. The nonlinear character of the rate law, if any, will then appear in the variation of $\Delta G_{f,p}^{\ddagger}$ with the peak potential, which provides a point-by-point depiction of the activation driving force relationship (one point per scan rate). The nonlinear character

of the rate law will also transpire in the variation of α_p, derived from

$$\alpha_p = 1.857\frac{\mathcal{R}T}{F(E_{p/2} - E_p)}$$

with the scan rate.

(ii) If the nonlinear character of the kinetic law is more pronounced, and/or if more data points than merely the peak are to be processed, the convolution approach[21] may be used, as sketched in Figure 7. One starts from the general expression of the rate law (eq 1), before any particular form has been stipulated for the function $k_f(E)$. Noting that

$$(C_A)_{x=0} + (C_B)_{x=0} = C^0$$

eq 1 becomes

$$\frac{i}{FSC^0} = k_f(E)\left[1 - \frac{(C_B)_{x=0}}{C^0}\left\{1 + \exp\left[\frac{F}{\mathcal{R}T}(E - E^0)\right]\right\}\right]$$

Combination of these two equations allows the derivation of the forward rate constant as a function of the electrode potential and, knowing the standard potential of the A/B couple, also rate constant of the backward reaction. The example selected to illustrate the extraction of the kinetic law from the cyclic voltammetric raw data in Figure 6 is an adiabatic electron-transfer obeying MHL kinetics with a maximal rate constant, $k_\infty = 4 \times 10^3$ cm s^{-1} and a reorganization energy $\lambda = 1.4$ eV, thus implying (eq 7) that $k_S = 8.4 \times 10^{-4}$ cm s^{-1}.

The convolution treatment of the linear and semi-infinite diffusion reactant transport leads to the following relationship between the concentrations at the electrode surface and the current:

$$1 - \frac{(C_A)_0}{C^0} = \frac{(C_B)_0}{C^0} = \frac{1}{\sqrt{\pi}}\int_0^t \frac{\sqrt{Fv/\mathcal{R}T}}{FSC^0\sqrt{D}}\frac{i(\eta)}{\sqrt{t-\eta}}\,d\eta$$

Variation of the scan rate over the maximal available range (0.1−10^6 V/s) allows the investigation of the kinetic law over a rather extended range of driving forces (Figure 7), which, however, does not allow the maximal rate constant region to be reached. The example selected to illustrate the immobilized reactant case (Figure 4) was easier to deal with, leading to a more complete coverage of the activation-driving force relationship thanks to the lower values of the rate constant due to the strong nonadiabaticity of the reaction.

The preceding derivation has assumed implicitly that the double layer charging current is negligible in front of the faradaic current or that it can be eliminated by a simple subtraction procedure. In cases where these conditions are not fulfilled, the following treatment will take care of the problem under the assumption that the double layer capacitance is not appreciably affected by the faradaic reaction but may nevertheless vary in the potential range explored. The first step of the treatment consists of extracting the faradaic component from the total current according to eq 13, after the double layer capacitance has been determined in a blank experiment. The previously described procedure is then applied to the faradaic current thus extracted from the raw data.

In total, we see that, in the immobilized case as well as in the free-moving case, the cyclic voltammetric examination of the electron-transfer kinetics does not require the a priori knowledge of the rate law.

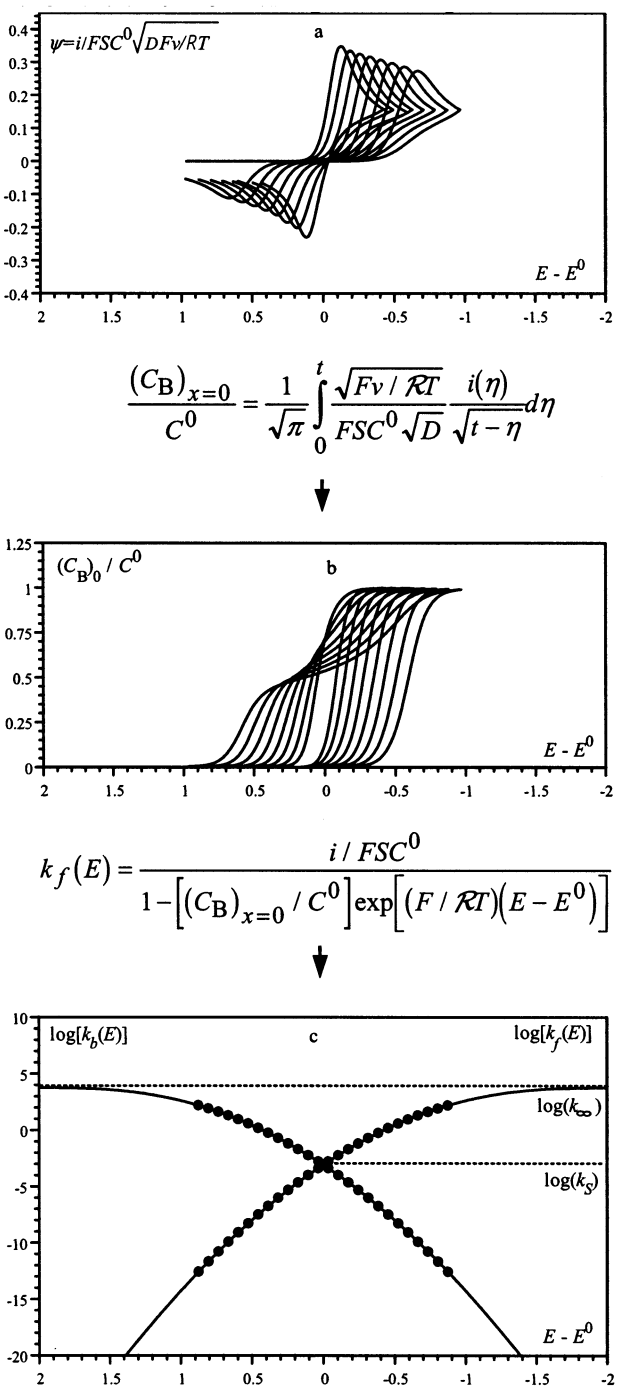

Figure 7. Deriving the rate law of an electron-transfer involving free moving reactants from the cyclic voltammetric responses. (a) Voltammograms recorded at 0.1, 1, 10, 100, 1000, 10 000, 100 000, 1 000 000 V/s. (b) Derivation of the surface concentrations from convolution of the current responses. (c) Potential-dependent rate constants (cm/s) from the combination of a and b. In this example, the outcome of the analysis is an adiabatic MHL kinetics with $\lambda = 1.4$ eV, $k_\infty = 4 \times 10^3$, $k_S = 8.4 \times 10^{-4}$ cm/s.

Evidencing the Variation of the Transfer Coefficient with the Electrode Potential

A good example of such a variation in the attached case is provided by the kinetics of the ferrocene/ferrocenium couple attached to a gold electrode by a long chain alkanethiol assembled together with unsubstituted alkanethiols of similar

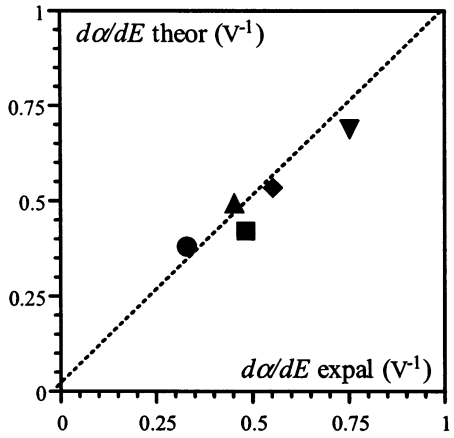

Figure 8. Variations of the transfer coefficient with the electrode potential derived from convolutive cyclic voltammetry of the following systems (data from ref 8).

length.[5] The reaction is expected to be nonadiabatic owing to the large distance between the reactant and the electrode surface. The situation is closely similar to the example shown in Figure 4. The smallness of the standard rate constant, k_S, caused by the strong nonadiabaticity of the reaction allowed an easy characterization of the kinetics over a large range of driving forces, resulting in a particularly clear demonstration of the nonlinear character of the activation/ driving force law.

The adiabatic reduction of a series of nitro compounds in acetonitrile or DMF solutions[5] provides examples of nonlinear activation/driving force relationships. Convolution of the cyclic voltammetric data was employed, as described in Figure 7, both to avoid the a priori stipulation of the rate law and to cover the maximal range of electrode potentials varying the scan rate and using the whole curve, and not merely the peak, for each scan rate. In the range of driving force available in these studies, the MHL model predicts a practically linear potential dependence of α. This is what is found experimentally with values of the rate of variation, dα/dE, which are those summarized in Figure 8. The values of dα/dE predicted by the MHL model may be derived from the values of the standard rate constant. The two sets of values are compared in Figure 8, with correction of the double layer, showing that there is a good agreement between theory and experiment.

Appendix

Derivation of Equations 4, 6, and 7.

$$\frac{k_f}{k_\infty} = \frac{\int_{-\infty}^{\infty} \kappa_{el}(\mathbf{E})\,\rho(\mathbf{E}) \dfrac{\exp\left[-\dfrac{F}{4\mathcal{R}T\lambda}[\lambda - (\mathbf{E}-\mathbf{E}^0)]^2\right]}{1+\exp\left[\dfrac{F}{\mathcal{R}T}(\mathbf{E}-\mathbf{E}_F)\right]}\,d\mathbf{E}}{\lim(\mathbf{E}_F-\mathbf{E}^0\gg\lambda)\int_{-\infty}^{\infty} \kappa_{el}(\mathbf{E})\,\rho(\mathbf{E}) \dfrac{\exp\left[-\dfrac{F}{4\mathcal{R}T\lambda}[\lambda - (\mathbf{E}-\mathbf{E}^0)]^2\right]}{1+\exp\left[\dfrac{F}{\mathcal{R}T}(\mathbf{E}-\mathbf{E}_F)\right]}\,dE}$$

where k_∞ is the maximal rate constant and $\rho(E)$ is the density of states corresponding to the energy E.

Similarly, for the oxidation process

$$\frac{k_b}{k_\infty} = \frac{\int_{-\infty}^{\infty} \kappa_{el}(\mathbf{E})\,\rho(\mathbf{E}) \dfrac{\exp\left[-\dfrac{F}{4\mathcal{R}T\lambda}[+(\mathbf{E}-\mathbf{E}^0)]^2\right]}{1+\exp\left(-\dfrac{\mathbf{E}-\mathbf{E}_F}{\mathcal{R}T}\right)}\,dE}{\lim(\mathbf{E}_F-\mathbf{E}^0\ll\lambda)\int_{-\infty}^{\infty} \kappa_{el}(\mathbf{E})\,\rho(\mathbf{E}) \dfrac{\exp\left[-\dfrac{F}{4\mathcal{R}T\lambda}[\lambda + (\mathbf{E}-\mathbf{E}^0)]^2\right]}{1+\exp\left(-\dfrac{\mathbf{E}-\mathbf{E}_F}{\mathcal{R}T}\right)}\,dE}$$

Assuming, as discussed in the text, that ρ and κ_{el} are independent of E and introducing

$$\zeta = F\frac{\mathbf{E}-\mathbf{E}_F}{T}$$

$$\frac{k_f}{k_\infty} = \frac{\int_{-\infty}^{\infty} \dfrac{\exp\left[-\dfrac{\mathcal{R}T}{4F\lambda}\left\{\dfrac{F}{\mathcal{R}T}[\lambda + (E-E^0)] - \zeta\right\}^2\right]}{1+\exp(\zeta)}\,d\zeta}{\lim(E-E^0\gg\lambda)\int_{-\infty}^{\infty} \dfrac{\exp\left[-\dfrac{\mathcal{R}T}{4F\lambda}\left\{\dfrac{F}{\mathcal{R}T}[\lambda + (E-E^0)] - \zeta\right\}^2\right]}{1+\exp(\zeta)}\,d\zeta}$$

Likewise, introducing

$$\zeta = -F\frac{\mathbf{E}-\mathbf{E}_F}{T}$$

$$\frac{k_b}{k_\infty} = \frac{\int_{-\infty}^{\infty} \dfrac{\exp\left[-\dfrac{\mathcal{R}T}{4F\lambda}\left\{\dfrac{F}{\mathcal{R}T}[\lambda - (E-E^0)] - \zeta\right\}^2\right]}{1+\exp(\zeta)}\,d\zeta}{\lim(E-E^0\gg\lambda)\int_{-\infty}^{\infty} \dfrac{\exp\left[-\dfrac{\mathcal{R}T}{4F\lambda}\left\{\dfrac{F}{\mathcal{R}T}[\lambda - (E-E^0)] - \zeta\right\}^2\right]}{1+\exp(\zeta)}\,d\zeta}$$

an alternative change of integration variable is as follows:

$$v = \frac{\zeta - \dfrac{F}{\mathcal{R}T}[\lambda + (E-E^0)]}{\sqrt{4\dfrac{F\lambda}{T}}}$$

leading to

$$\frac{k_f}{k_\infty} = \frac{\int_{-\infty}^{\infty} \dfrac{\exp(-v^2)\,dv}{1+\exp\left\{\dfrac{F}{\mathcal{R}T}[\lambda + (E-E^0)]\right\}\exp\left(\sqrt{4\lambda\dfrac{F}{\mathcal{R}T}}v\right)}}{\lim(E-E^0\ll\lambda)\int_{-\infty}^{\infty} \dfrac{\exp(-v^2)\,dv}{1+\exp\left\{\dfrac{F}{\mathcal{R}T}[\lambda + (E-E^0)]\right\}\exp\left(\sqrt{4\lambda\dfrac{F}{\mathcal{R}T}}v\right)}}$$

The denominator may be computed as follows.

$\lim(E-E^0 \ll \lambda)$

$$\int_{-\infty}^{\infty} \frac{\exp(-v^2)\,dv}{1+\exp\left\{\frac{F}{\mathcal{R}T}[\lambda+(E-E^0)]\right\}\exp\left(\sqrt{4\lambda\frac{F}{\mathcal{R}T}}v\right)} = \int_{-\infty}^{\infty}\exp(-v^2)\,dv = \sqrt{\pi}$$

And thus

$$\frac{k_f}{k_\infty} = \frac{1}{\sqrt{\pi}}\int_{-\infty}^{\infty} \frac{\exp(-v^2)\,dv}{1+\exp\left\{\frac{F}{\mathcal{R}T}[\lambda+(E-E^0)]\right\}\exp\left(\sqrt{4\lambda\frac{F}{\mathcal{R}T}}v\right)}$$

Likewise

$$\frac{k_b}{k_\infty} = \frac{1}{\sqrt{\pi}}\int_{-\infty}^{\infty} \frac{\exp(-v^2)\,dv}{1+\exp\left\{\frac{F}{\mathcal{R}T}[\lambda-(E-E^0)]\right\}\exp(\sqrt{4\lambda}v)}$$

with

$$k_\infty = Z^{el}\kappa_{el}$$

At zero driving force ($E = E^0$): $k_f = k_b = k_S$, with

$$\frac{k_S}{k_\infty} = \frac{1}{\sqrt{\pi}}\int_{-\infty}^{\infty} \frac{\exp(-v^2)\,dv}{1+\exp\left(\frac{F\lambda}{\mathcal{R}T}\right)\exp(\sqrt{4\lambda}v)}$$

The expressions of the rate constants given in eqs 4, 6, and 7 ensue.

References and Notes

(1) (a) Levich, V. G. Present State of the Theory of Oxidation−Reduction in Solution (Bulk and Electrode Reactions). In *Advances in Electrochemistry and Electrochemical Engineering*; Delahay, P., Tobias, C. W., Eds.; Wiley: New York, 1966; pp 250−371. (b) Hale, J. M. *J. Electroanal. Chem.* **1968**, *19*, 315. (c) Hush, N. S. *J. Electroanal Chem.* **1999**, *470*, 170.

(2) (a) Marcus, R. A. *J. Chem. Phys*. **1956**, *24*, 4966. (b) Marcus, R. A. *J. Chem. Phys*. **1965**, *43*, 679. (c) Marcus, R. A. *Electrochim. Acta* **1968**, *13*, 955.

(3) (a) Hush, N. S. *J. Chem. Phys*. **1958**, *28*, 962. (b) Hush, N. S. *Electrochim. Acta* **1968**, *13*, 1005.

(4) Finklea, H. O. In *Electronalytical Chemistry*; Bard, A. J., Rubinstein, I., Eds.; Dekker: New York, 1996; Vol. 19.

(5) Chidsey, C. E. D. *Science* **1991**, *251*, 919.

(6) Bard, A. J.; Faulkner, L. R. *Electrochemical Methods*; Wiley: New York, 2001; pp 124−132.

(7) Gosavi, S.; Marcus, R. A. *J. Phys Chem. B* **2000**, *104*, 2067.

(8) Savéant, J.-M.; Tessier. D. *Faraday Discuss. Chem. Soc*. **1982**, *74*, 57.

(9) (a) Antonello, S.; Maran, F. *J. Am. Chem. Soc*. **1999**, *121*, 9668. (b) Savéant, J.-M. Electron Transfer, Bond Breaking and Bond Formation. In *Advances in Physical Organic Chemistry;* Tidwell, T. T., Ed.; Academic Press: New York, 2000; Vol. 35, pp 117−192.

(10) Finklea, H. O. *J. Phys. Chem. B* **2001**, *105*, 8685.

(11) Finklea, H. O. *J. Electroanal Chem.* **2001**, *495*, 79.

(12) Sutin, N. *Prog. Inorg. Chem. Soc*. **1983**, *30*, 441.

(13) (a) Savéant, J.-M. *J. Am. Chem. Soc*. **1987**, *109*, 6788. (b) Savéant, J.-M. *J. Am. Chem. Soc.* **1992**, *114*, 10595. (c) Andrieux, C. P.; Savéant, J.-M.; Tardy, C.; Savéant, J.-M. *J. Am. Chem. Soc.* **1998**, *120*, 4167.

(14) (a) Brunschwig, B. S.; Logan, J.; Newton, M. D.; Sutin, N. *J. Am. Chem. Soc*. **1980**, *102*, 5798. (b) Newton, M. D.; Sutin, N. *Annu. Rev. Phys. Chem.* **1984**, *35*, 437.

(15) (a) Landau, L. *Phys. Z. Sowjet* **1932**, *2*, 46. (b) Zener, C. *Proc. R. Soc., London Ser. A* **1932**, *137*, 696.

(16) Taking kT/h for the nuclear frequency, referring all energies to one mole and expressing them in electronvolts. The average distance over which the electron transfer takes place is correspondingly given by $\delta_{el} = h/\sqrt{2\pi mkT}$, m being the molecular mass).

(17) Newton, M. D.; Sutin, N. *Annu. Rev. Phys. Chem.* **1984**, *35*, 437.

(18) Delahay, P. *Double Layer and Electrode Kinetics*; Wiley: New York, 1965.

(19) Laviron, E. *J. Electroanal Chem.* **1979**, *101*, 19.

(20) (a) Matsuda, H.; Ayabe, Y. *Z. Elektrochem*. **1955**, *59*, 494. (b) Nadjo, L. Savéant, J.-M. *J. Electroanal. Chem.* **1973**, *48*, 113.

(21) (a) Andrieux, C. P.; Savéant, J.-M. *J. Electroanal. Chem.* **1970**, *26*, 147. (b) Imbeaux, J. C.; Savéant, J.-M. *J. Electroanal. Chem.* **1973**, *44*, 169. (c) Savéant, J.-M.; Tessier, D. *J. Electroanal. Chem*. **1975**, *65*, 57.